Available online at www.sciencedirect.com
SCIENCE DIRECT®
International Journal of Heat and Mass Transfer 47 (2004) 3943–3955
International Journal of HEAT and MASS TRANSFER
www.elsevier.com/locate/ijhmt

Minimum gas speed in heat exchangers to avoid particulate fouling

M.S. Abd-Elhady [a,*], C.C.M. Rindt [a], J.G. Wijers [b], A.A. van Steenhoven [a], E.A. Bramer [c], Th.H. van der Meer [c]

[a] Department of Mechanical Engineering, Eindhoven University of Technology, W-Hoog 3.144, P.O. Box 513, 5600 MB Eindhoven, The Netherlands

[b] Department of Chemical Engineering, Eindhoven University of Technology, P.O. Box 513, 5600 MB Eindhoven, The Netherlands

[c] Department of Mechanical Engineering, University of Twente, P.O. Box 217, 7500 AE Enschede, The Netherlands

Received 28 October 2003; received in revised form 19 January 2004
Available online 13 May 2004

Abstract

The minimum gas speed for a heat exchanger (HE) at which particulate fouling is avoided is investigated. Fouling experiments have been done with particles of different sizes and different materials running under different gas speeds. It is found that the smallest particles in the flow deposit first on the tubes of the HE at areas of minimum flow velocities. Then the large particles deposit and the fouling layer starts to build up. The fouling layer thickness and growth over the HE tube is influenced by the flow speed. As the flow speed in the HE increases, the thickness and the surface area of the fouling layer deposited over the heat exchanger tube are reduced. There is a limiting flow speed above which fouling is avoided. This limiting speed is related to the critical flow velocity required to roll a particle resting on a flat surface. To prevent fouling, the gas speed of a HE should be larger than the critical flow velocity that corresponds to the particle size most likely to stick on the heat exchanger tube.

Keywords: Particulate; Fouling; Heat exchanger

1. Introduction

Particulate fouling is defined as the deposition of unwanted material (particles) on a heat exchange surface. Fouling can lead to increased capital and maintenance costs and major production and energy losses in many energy-intensive industries, Taborek et al. [1]. In this study attention is given to the design of heat exchangers based on limiting particulate fouling. The objective of this research is to find the minimum gas speed for a heat exchanger at which particulate fouling is avoided.

Müller-Steinhagen et al. [2] and Grillot and Icart [3] have shown that when the gas speed in a heat exchanger is increased particulate fouling is reduced. Cabrejos and Klinzing [4] have shown that increasing the flow speed in circular ducts to a certain limit can prevent particles in the flow from sedimentation on the bottom of the tube or can pick up particles that have already been deposited. The minimal flow speed required to roll a particle resting on a flat surface is called the critical flow speed. The critical flow speed is a function of the flue gas kinematic viscosity and the resting particle material and diameter. Abd-Elhady et al. [5] have shown that the critical flow velocity decreases with the increase of the resting particle diameter and with the decrease of the

* Corresponding author. Tel.: +31-402-473172; fax: +31-402-433445.
E-mail address: m.s.abdelhady@tue.nl (M.S. Abd-Elhady).

0017-9310/$ - see front matter © 2004 Elsevier Ltd. All rights reserved.
doi:10.1016/j.ijheatmasstransfer.2004.03.024

Nomenclature

D	particle diameter, m
d	contact diameter, m
d_{cy}	cylinder diameter, m
e	coefficient of restitution
F_d	drag force, N
F_L	lift force, N
F_b	buoyancy force, N
F_a	adhesion force, N
F_g	gravity force, N
HE	heat exchanger
m	particle mass, kg
PSD	particle size distribution
Q_k	particle kinetic energy, J
Q_E	particle elastic energy, J
Q_L	particle dissipated energy, J
Q_A	adhesive energy between a particle and a substrate during approach, J
Q'_A	adhesive energy between a particle and a substrate during restitution, J
R	particle radius, m
Re	Reynolds number
SEM	scanning electron microscope
U	velocity in x direction, m/s
V	velocity in y direction, m/s
V_{im}	normal impact speed, m/s
V_r	normal rebound speed, m/s

Greek symbols

α	particle radius of deformation, m
ε	rate of turbulent energy dissipation per unit mass, m^2/s^3
k	turbulent kinetic energy, J

Subscripts

A, a	adhesion
b	buoyancy
cy	cylinder
d	drag
E	elastic
g	gravity
im	impact
k	kinetic
L	lift, lost
r	rebound

flue gas kinematic viscosity. The influence of gas speed, critical flow velocity, diameter and material of the particles suspended in the flue gases on fouling of heat exchangers are investigated experimentally.

Heat exchangers in low temperature applications such as the economizers of boilers are subjected to gases that contain a wide range of particle sizes. To prevent fouling of heat exchangers based on the critical flow velocity, the critical flow velocity should be selected based on the particle size most likely to stick first to the heat exchanger tubes. Van Beek [6] has reported that the fouling layer found on the economizer tubes of a boiler contained particles with sizes ranging from 1 to 10 μm. This range represented only a small portion of the fly ash particle sizes in the flue gases that contained particles with sizes ranging from 1 to 450 μm. Müller-Steinhagen et al. [2] investigated the deposition of alumina particles onto a heat transfer surface using two fouling probes, a heated cylindrical rod in an annulus and a coiled wire in cross-flow. Müller-Steinhagen found that the fouling layers contained particles with an average diameter of 0.45 μm resulting from particles with an average diameter of 2 μm suspended in the flow. Rogers and Reed [7] and Fichman and Pnueli [8] both introduced an elastic–plastic impact model. It provides a criterion for the adhesion or rebound of a particle impacting a solid surface as function of the particle impact velocity and the material properties of both the particle and the surface. In the present study, the Rogers and Reed model is solved to determine which particle size is likely to stick first from a batch of particles hitting a flat solid surface. Then experimental results are shown to determine which particle size deposits first from a batch of particle sizes flowing over a heat exchanger tube. A comparison is made between the experimental results and Rogers and Reed model results. The fouling layers found on the heat exchanger tubes are examined to see the influence of heat on the fouling layer structure. Based on the results, recommendations are given for the design of heat exchangers.

2. Experimental setup and experimental procedure

An experimental setup has been built and developed to study the mechanism of fouling as a function of flow speed and contaminating particles. The setup as shown in Fig. 1a consists of an air heater, particle feeder, heat exchanger and an exhaust system. A 5-bar air supply is connected to the setup. The airflow rate is controlled by a critical nozzle and a pressure regulator. The air temperature is controlled via an air heater of 30 kW. The air heater can heat air from room temperature to 500 °C with a maximum airflow rate of 0.05 m^3/s. Particles of known size are added to the airflow before the air is passed to the heat exchanger. Two types of particles are

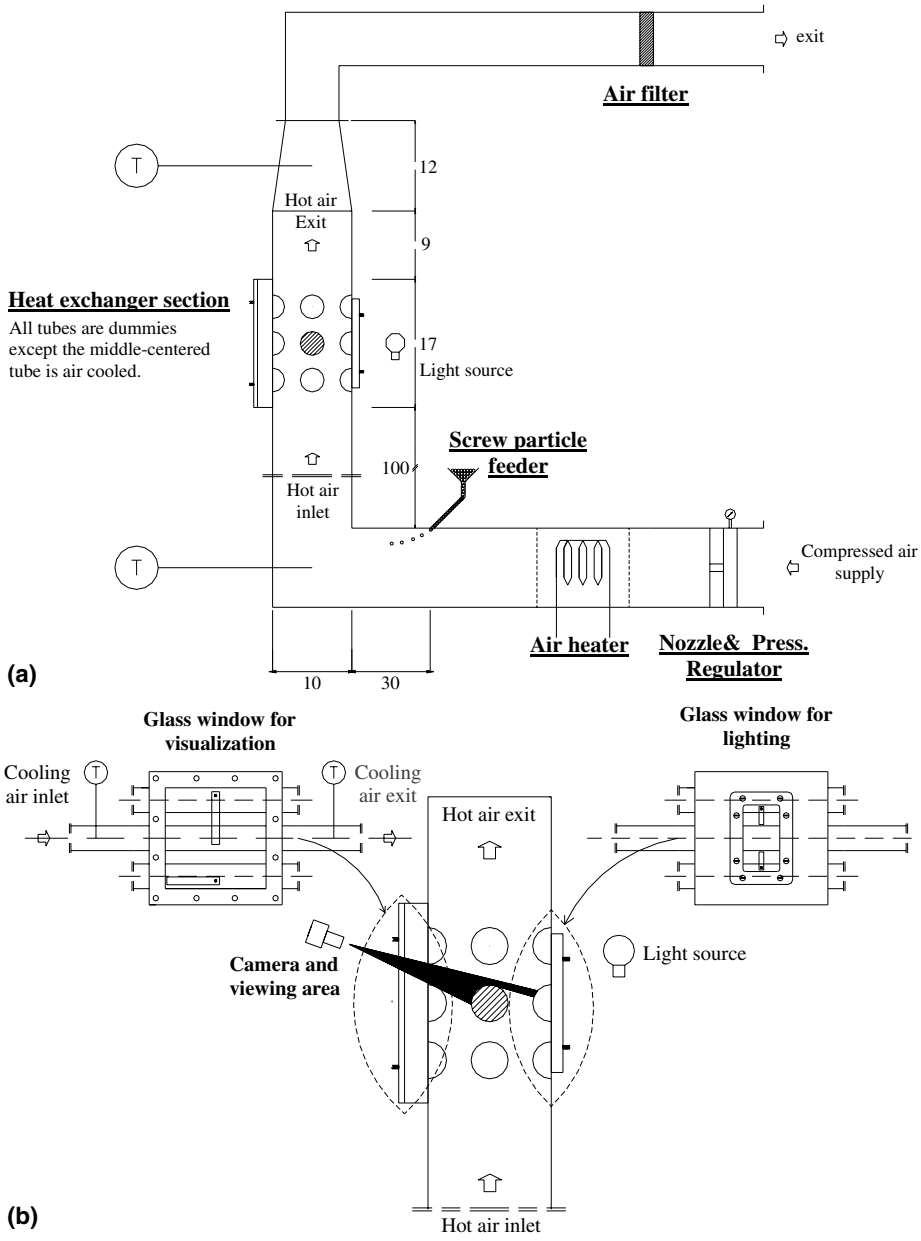

Fig. 1. (a) A schematic diagram of the experimental setup. (b) The heat exchanger section showing the tube area viewed by the camera and also the two glass windows installed for visualization and lighting. All dimensions are in cm.

used in the fouling experiments, non-metallic spherical glass particles and metallic spherical bronze and copper particles. The glass particles have an average diameter of 21 μm with a standard deviation of 16 μm. The copper particles have an average diameter of 10 μm with a standard deviation of 5 μm, while the spherical bronze particles have an average diameter of 55 μm with a standard deviation of 6 μm. Particle size distributions (PSD) and scanning electron microscope (SEM) photos for the glass, copper and bronze particles used in the experiments are shown in Fig. 2. Particles are supplied to the airflow through a screw feeder. The injection rate of particles is controlled through the rotational speed of the feeder screw. The heat exchanger section consists of three tubes and six half tubes made of stainless steel and of outer diameter 3.16 cm installed as shown in Fig. 1a. Only the middle centered tube in the heat exchanger section is cooled internally by air at room temperature.

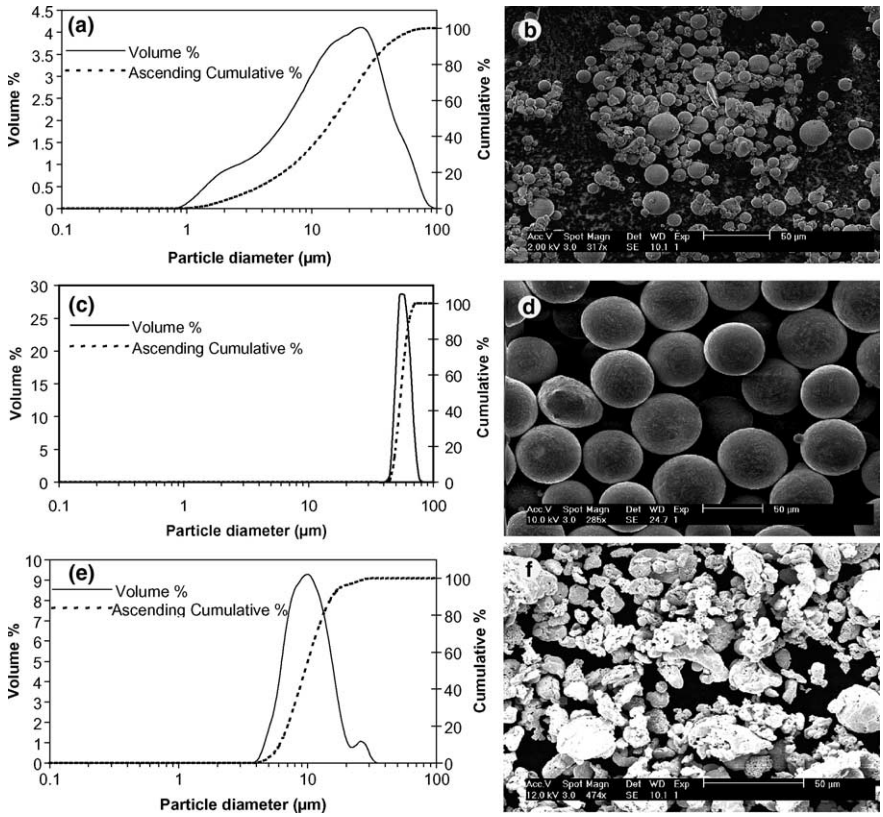

Fig. 2. Particle size distributions (PSD, left) and scanning electron microscope (SEM, right) photos of glass (a,b), bronze (c,d) and copper particles (e,f), respectively.

The cooling airflow rate is also controlled through a critical nozzle and a pressure regulator.

Fouling of the heat exchanger tube is monitored using a digital camera through a glass window installed in the heat exchanger section as shown in Fig. 1b. The digital camera is the Finepix S602 zoom, with a resolution of 2832 pixels × 2128 pixels, i.e. 6.03 million pixels. The digital camera has a 6× optical zoom which compared to small image format has a zoom area of 35–210 mm. The fouling layer thickness is measured optically. Images are taken of the heat exchanger tubes before and during fouling. The clean heat exchanger tube radius is taken as a reference. The tube radii in the camera images and hence the fouling layer thicknesses are determined with an accuracy of ±1 pixel which corresponds to ±0.04 mm. The temperatures of the hot air and the cooling air before and after the heat exchanger are measured using K type thermocouples with an accuracy of ±0.4 °C. The air speed at the exit of the heat exchanger section is measured by a hot wire anemometer with an accuracy of ±0.015 m/s. Air exhaust from the setup is filtered through a bag filter before it goes into the atmosphere.

Each fouling experiment is carried out in the following procedure: Hot and cold airflow rates are adjusted to the desired flow rates at the beginning of the experiment. The hot air temperature is adjusted through the air heater and the experiment is kept running till a steady state is reached. After a steady state has been reached, particles are injected at the desired rate and the fouling process is monitored.

3. Results and discussion

3.1. Influence of flow speed on growth of fouling layer

The following experiments are performed to see the influence of flow speed on the growth of the fouling layer and to determine the flow speed at which fouling ceases. Two types of particles are used in the experiments, the non-metallic glass particles and the metallic bronze and copper particles defined in the previous section.

In the first experiments, glass particles have been injected in the flow at different gas flow speeds and the fouling behavior is monitored. The average airflow speed between the tubes has been changed from 2.7 to 3.8 to 5 m/s and in each case the operating time was 9 h. The air temperature is 200 °C and the particles

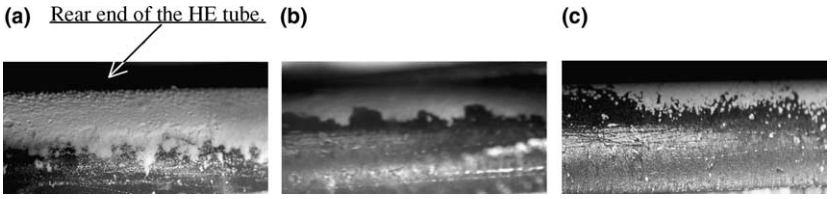

Fig. 3. Fouling layer at the end of 9 h of operation for different flow speeds. The foulant is spherical glass particles of diameter 21 ± 16 μm. (a) $V = 2.7$ m/s; (b) $V = 3.8$ m/s; (c) $V = 5$ m/s.

Table 1
Comparison between the fouling behaviors for glass particles under different operating conditions

Average airflow speed between the HE tubes	$V = 2.7$ m/s	$V = 3.8$ m/s	$V = 5$ m/s
Final thickness (mm)	1	0.75	0.3
Circumferential and radial growth	Continues	Starts very fast and then decreases abruptly	Starts very fast and then decreases abruptly

concentration is 0.15 g/N m^3 of flowing air. Fig. 3 shows the fouling layer at the end of operation for the above-mentioned cases. Table 1 shows a comparison between the three different cases. It is shown that as the speed of the flow increases, the fouling layer surface area and thickness are reduced. Increasing the average air speed between the heat exchanger (HE) tubes from 2.7 to 5 m/s reduces the final fouling layer thickness from 1 to 0.3 mm after 9 h of operation. When the average flow speed between the HE tubes is 2.7 m/s, it is found that the circumferential and radial growth of the fouling layer continued from the beginning till the end of the experiment. Increasing the average flow speed between the HE tubes to 3.8 and 5 m/s showed a different fouling behavior. The fouling rate was very high at the beginning, especially for the first 3 h. Then the fouling rate started to decrease abruptly for the next 6 h of operation, till hardly any radial or circumferential growth can be seen.

Figs. 4 and 5 show the growth of the fouling layer for glass particles over the heat exchanger tube as a function of time. The average air speed between the tubes is 2.7 m/s for Fig. 4 and 3.8 m/s for Fig. 5. Fig. 4a shows that at the beginning of the fouling process, some particles start to deposit at intermittent and distant positions. These points of deposition start to grow radially, Fig. 4b–e, till the whole surface of the heat exchanger tube is covered completely with particles, Fig. 4f. The surficial growth of the fouling layer is emphasized by the encircled areas in Figs. 4a–f. The surficial growth of the fouling layer can be explained by the fact that fine particles are most likely to stick first to the HE tubes because of their higher sticking velocity compared to coarse particles [7]. Then larger particles, which deposit on the heat exchanger tube and stand alone in the shearing flow, start to roll over the heat exchanger tube if the shearing flow speed is above a certain limit. The particle rolling motion is stopped when it is blocked by a standing heap of particles, which leads to the surficial growth of the fouled areas till they cover the unfouled surfaces. The flow speed required to roll a particle resting on a flat surface, and, the sticking velocity of a particle, will respectively be discussed in detail in the following subsequent sections.

Fig. 5 shows that at the beginning of the fouling experiment, Fig. 5b, the glass particles in the flow started to deposit on the rear end of the HE tube and continued to the circumference, Fig. 5c–e. The rear end of the heat exchanger, Fig. 5f, is subjected to the lowest shearing forces due to separation of flow from the tube surface, Achenbach [9]. The flow field for the examined HE shown in Fig. 1 is solved using the finite volume method applied by the commercial CFD-package CFX version 4.2. The low Reynolds number k–ε model is used to solve the flow field around the HE tubes. For all but the advection terms, use is made of a second-order central differencing scheme. In the equations for the velocity components, use is made of the third order QUICK interpolation scheme for the advection terms. For the k and ε equations the first order HYDRID-scheme is applied which is more stable than the QUICK scheme and ensures the k and ε values to remain positive in the converged solution. In the computations use is made of the SIMPLEC pressure-correction scheme in which the pressure field is indirectly specified via the continuity equation. For the u and the v velocity use is made of the Stone's method, for the turbulence quantities a line-relaxation method is used and an algebraic multi-grid method is applied for the pressure equation. The flow field is solved for a turbulent flow, at $Re = 2 \times 10^5$, which

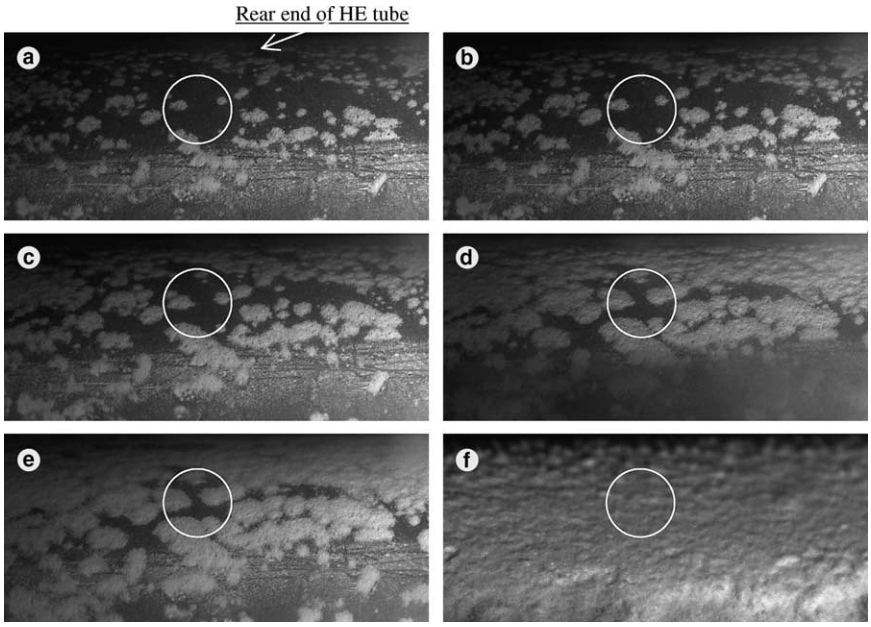

Fig. 4. Progress of the fouling layer over the HE tube within 9 h of operation. The foulant is spherical glass particles of diameter 21 ± 16 μm. The average air speed between the HE tubes is 2.7 m/s: (a) after 1 h of operation, (b) after 1.5 h of operation, (c) after 2 h of operation, (d) after 2.5 h of operation, (e) after 3 h of operation, (f) after 9 h of operation.

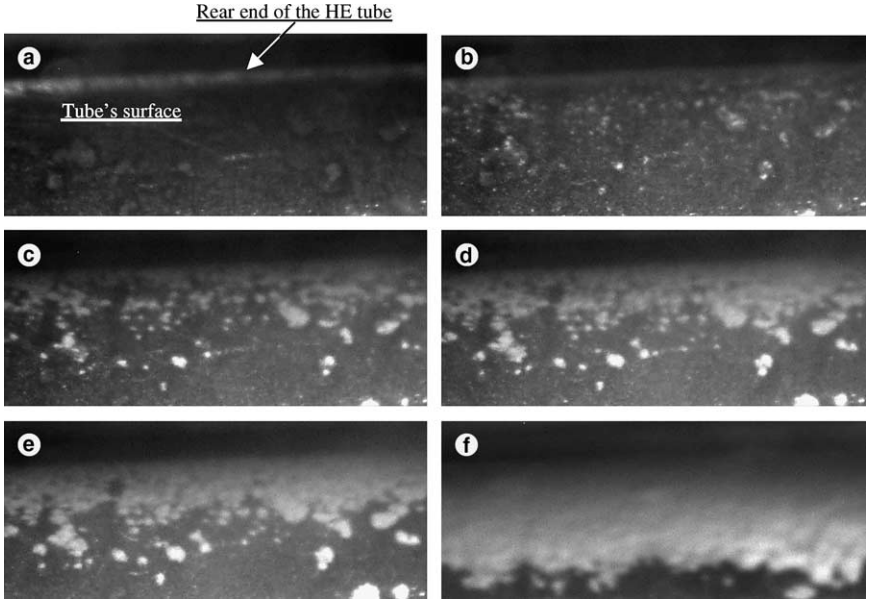

Fig. 5. Growth of the fouling layer over the HE tube within 6 h of operation. The foulant is spherical glass particles of diameter 21 ± 16 μm. The average air speed between the tubes is 3.8 m/s: (a) at the beginning, (b) after 0.5 h of operation, (c) after 1 h of operation, (d) after 1.5 h of operation, (e) after 2 h of operation, (f) after 6 h of operation.

corresponds to a superficial flow velocity of 10 m/s. Fig. 7 shows the velocity contours in the y and x directions for the HE shown in Fig. 1. Although the CFD calculations show that the flow around the middle centered tube is not periodic, this centered tube can be regarded as a representative for a tube in a tube bundle. It is shown that for

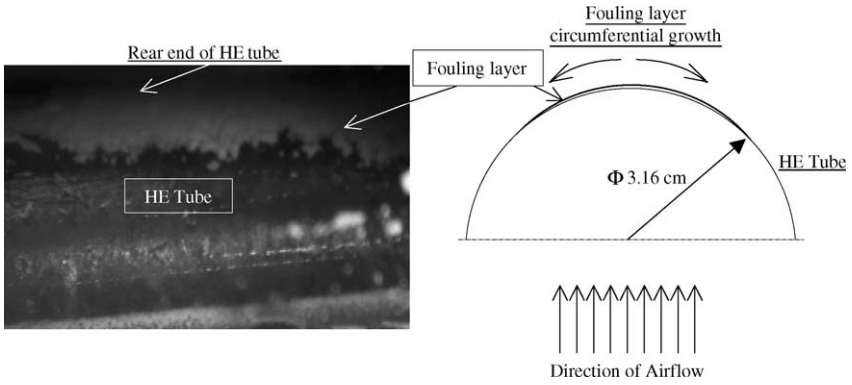

Fig. 6. A summary for the fouling layer circumferential growth shown in Fig. 5.

the middle centered tube the flow keeps attached to the tube surface and then separates at an angle of 120° from the stagnation point. From the numerical results it could also be concluded that there is more air circulation at the front than in the rear end of the middle centered HE tube, Fig. 7c and d. Therefore particles that stick to the rear end of the HE tube are more likely to remain in position than particles that stick to the sides of the HE tube. A particle that sticks to the side of the HE tube rolls over the HE tube if the airflow speed is above a certain limit, and stops if it is blocked by the resting particles at the rear end of the heat exchanger tube. Therefore fouling starts at areas that are subjected to minimum shearing forces and then spreads due to particle transport to the already deposited particles. Fig. 6 summarizes the circumferential growth of the fouling layer shown in Fig. 5.

3.2. Limiting fouling speed

The previous set of experiments has shown that as the flow speed in the HE increases, the thickness and the surface area of the fouling layer deposited over the HE tube are reduced. The following experiments are done to determine the flow speed at which fouling of the heat exchanger is prevented. The results of the experiment will be compared to the results achieved with an analytical model. The analytical model is only valid for spherical non-charged particles. The analytical model is based on the minimum shear velocity required to roll a particle on a flat surface. It can be applied for a cylindrical tube if the particle diameter is much smaller than the cylinder diameter, as is the case here. The shear flow speed required to roll a particle deposited on a flat surface is called the critical flow velocity and it is a function of the particle material and size and the surface material. The critical flow velocity can be calculated when assuming that the hydrodynamic rolling moment due to the drag force, F_d, lift force, F_L, and buoyancy force, F_b, is greater than the resting adhesion moment due to the surface adhesion force, F_a, and the force of gravity, F_g. The ratio between the hydrodynamic rolling moment and the adhesion resting moment is defined by Zhang et al. [10] as RM and equal to

$$\mathrm{RM} = \frac{\text{Hydrodynamic rolling moment}}{\text{Adhesion resting moment}} = \frac{F_d \times (1.399R - \alpha)}{(F_a + F_g - F_b - F_L) \times d/2}, \quad (1)$$

where R, d and α are the particle radius, contact diameter and the particle radius of deformation, respectively. If the RM value is greater than 1, rolling will take place. Abd-Elhady et al. [5] have calculated the critical flow velocity for spherical copper particles of diameters ranging from 5 to 50 μm, the results are shown in Fig. 8. The main flow stream velocity, i.e. the critical flow velocity, required to roll a copper particle of 10 μm is 10.5 m/s while for a 50 μm copper particle this velocity is 4.5 m/s.

Due to the comparison with the analytical model presented above, in the experiments only spherical metallic particles are used. The HE is operated at different air flowing speeds and different particle sizes to determine the operating speed at which fouling is prevented as function of the particles size in the flow. The flow speed at which fouling is prevented, is investigated for copper particles of average diameter 10 μm with a standard deviation of 5 μm suspended in the airflow and also for bronze particles of average diameter 55 μm with a standard deviation of 6 μm. The air temperature is 20 °C and the particle concentration is 2 g/m^3 of airflow. The heat exchanger is kept running for 8 h in each experiment. Experimental results of the fouling experiment are plotted in Fig. 8. Fig. 8 shows that when air is contaminated with the copper particles of average diameter 10 μm the HE tubes fouled when the average flow speed between the tubes was lower than 9.5 m/s, i.e.

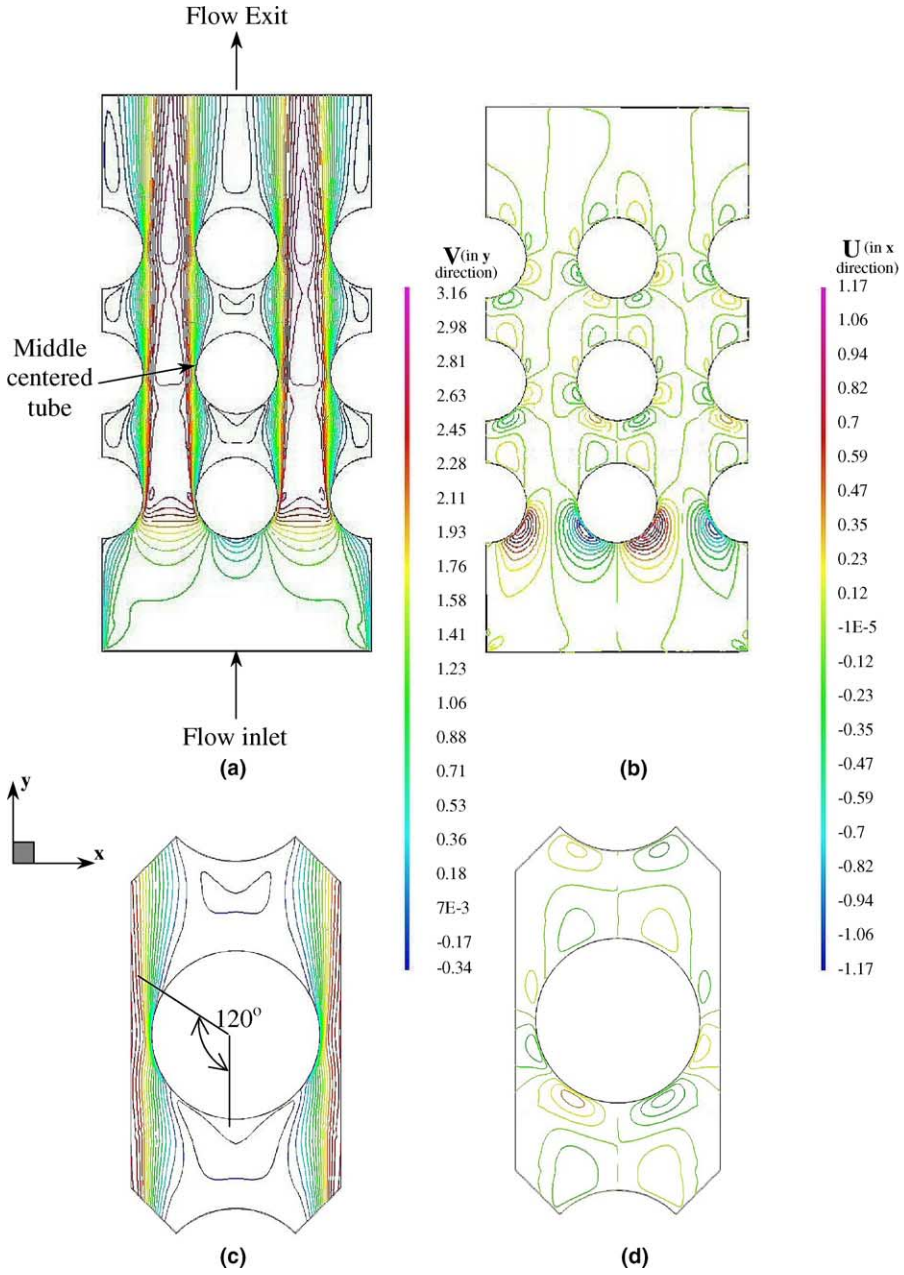

Fig. 7. Velocity contours in the y (left) and x (right) directions for the HE section (a,b) shown in Fig. 1b and for the middle centered tube (c,d), respectively. Reynolds number is 2×10^5.

7.5 and 2.7 m/s. It is also shown that when the air is contaminated with the bronze particles of average diameter 55 μm the HE tubes fouled when the average flow speed between the tubes was lower than 5.5 m/s, i.e. 4.5 and 2 m/s. Fig. 9 shows images for the HE tube at the end of the fouling experiments in case the airflow is contaminated with bronze particles of average diameter 55 μm. Fig. 9 shows that when the flow speed between the tubes is equal to 2 m/s the fouling layer thickness becomes 0.3 mm and diminishes when the flow speed becomes 5.5 m/s. The minimum flow speed at which fouling in a heat exchanger is prevented will be called the limiting fouling speed.

The copper particles used in the experiments have a wide particle size distribution ranging from 1 to 20 μm, as shown in Fig. 2e. Surprisingly, no fouling was found

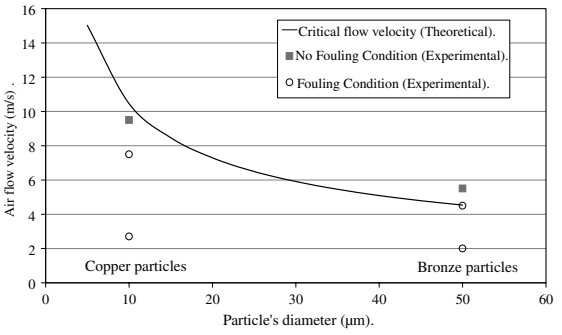

Fig. 8. The critical flow velocity and limiting fouling speed versus particle diameter.

of the copper particles smaller than 10 μm at a flow velocity of 9.5 m/s. This could be due to the small amount of the fine particles present and due to the removal of them by larger hitting particles. The removal of fine particles by the large depositing particles leads to a lower limiting fouling speed than the limiting fouling speed, which corresponds to the smallest particle in the gas flow. The effect of the particle size distribution on the fouling mechanism still has to be investigated.

The critical flow velocity shown in Fig. 8 is calculated for a metallic non-charged spherical copper particle resting on a good conductor surface. In case of an electrically charged particle resting on a bad conductor surface like glass an electrostatic adhesion force is developed which leads to a higher critical flow velocity than in case of a non-charged particle. The critical flow velocity then should be calculated based on the nature of the particles in the flow and the flow conditions.

3.3. Sticking of particles

In practical applications of heat exchangers especially in waste incinerators, the flue gases contain a wide range of particle sizes. To prevent fouling of heat exchangers based on the critical flow velocity, the critical flow velocity should be selected based on the particle size most likely to stick first to the heat exchanger tubes. The following experiments have been done to determine which particle size deposits first from a batch of particles flowing over a heat exchanger tube. A mixture of equal masses of bronze and copper particles is injected into the airflow. The bronze and copper particles used are defined in the experimental setup section. The particles concentration is 2 g/m^3 of airflow. Hot air at 200 °C and flow rate of 13E−3 N m^3/s is passed to the heat exchanger section. This results in a Reynolds number of 700 based on the HE tube diameter and the superficial flow velocity. An airflow rate of 1.5E−3 N m^3/s and a temperature of 20 °C was used for cooling the heat exchanger tube internally. The heat exchanger has run for 9 h. At the end of the fouling experiment samples are taken from the fouling layer deposited on the heat exchanger tube and these are examined by SEM. Two samples of particles are taken from the fouling layer deposited on the middle centered tube of the heat exchanger section: The first sample of particles was scratched from the top of the fouling layer. The second sample of particles was scratched from the first fouling layer of particles, which had deposited on the tube of the heat exchanger. This sample was taken by blowing air through the HE at a very high speed such that most of the fouling layer was blown off and only a very thin layer of particles remained on the tube of the heat exchanger. Fig. 10 shows SEM pictures for the particles at the bottom (near the heat exchanger tube) and at the top of the fouling layer respectively. First the fine copper particles have accumulated over the heat exchanger tube and then afterwards the larger bronze particles. The top of the fouling layer consisted mainly of the large bronze particles surrounded by the fine copper particles.

The same kind of experiment above is repeated using spherical glass particles instead of using a mixture of

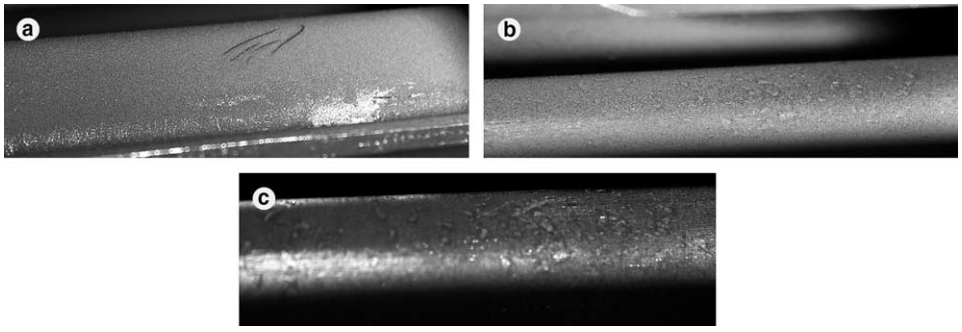

Fig. 9. Photos for the examined heat exchanger tube at the end of operation under different airflow velocities: (a) $V = 2$ m/s, a bronze layer of thickness 0.3 mm is formed on the HE steel tube; (b) $V = 4.5$ m/s, a very fine layer of bronze particles is formed; (c) $V = 5.5$ m/s, no fouling.

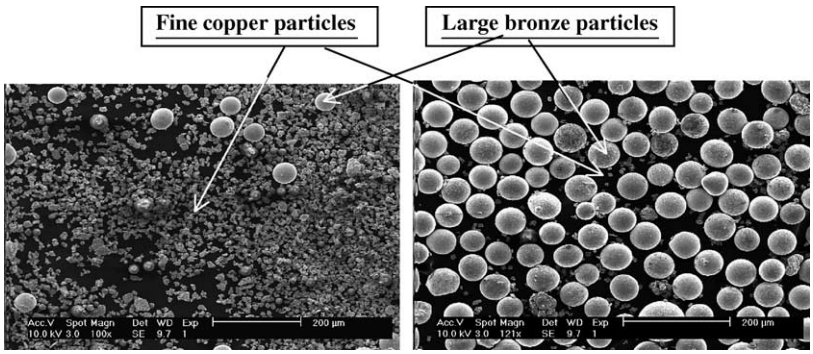

Fig. 10. Scanning electron microscope photos for the particles at the bottom (left) and top (right) of the fouling layer. The fouling layer is composed of a mixture of copper and bronze particles.

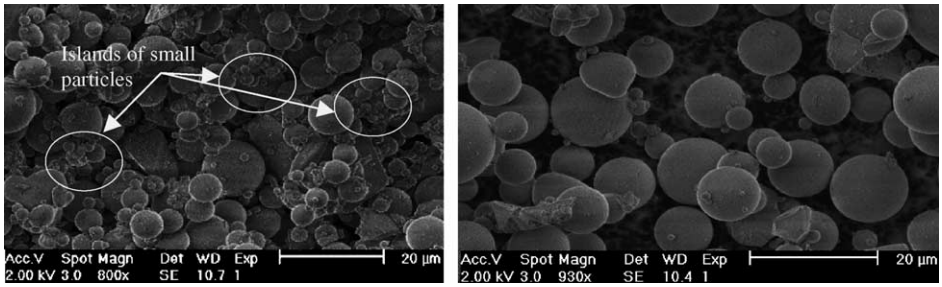

Fig. 11. Scanning electron microscope photos for the particles at the bottom (left) and top (right) of the fouling layer. The particles are made of glass.

bronze and copper particles. Fig. 11 shows SEM photos for the particles at the bottom (near the heat exchanger tube) and top of the fouling layer. At the top of the fouling layer large particles have accumulated with small particles in between. In the fouling layer near the tube of the heat exchanger, the finest particles in the flow have agglomerated together to form islands of fine particles connected to bigger particles. Fig. 12 and Table 2 show a comparison between the particles size distribution of the injected glass particles in the airflow and the glass particles in the fouling layer near the HE tube. It is shown that the average diameter of the glass particles has reduced from 20.4 μm in the airflow to 14.7 μm in the fouling layer near the HE tube. 90% of the injected glass particles in the airflow have a diameter less than 43.1 μm while 90% of the glass particles in the fouling layer near the HE tube have a diameter less than 25.2 μm. The reduction in particle size in the fouling layer near the HE tube from the particle size in the airflow is due to the higher sticking velocity of small particles compared to large particles as defined by Rogers and Reed [7].

Rogers and Reed [7] developed a model that describes the adhesion of a particle to a surface following an elastic–plastic impact. The model is based upon consideration of the energy balance during a normal impact between a sphere and a massive plane. The model describes the adhesion of a particle arising from only elastic deformations occurring during the approach of the particle to the surface. When the particle velocity is reduced to zero during the approach phase, part of the particle initial kinetic energy, Q_k, is converted into stored elastic energy, Q_E, while the remainder, Q_L, is dissipated. This is then followed by the recovery of the stored elastic energy, which is converted into kinetic energy of the rebounding particle. For a particle of mass m impacting a surface normally with a velocity V_{im} we have

$$\tfrac{1}{2}mV_{im}^2 + Q_A = Q_E + Q_L, \tag{2}$$

where Q_A is the energy due to the attractive forces between the incoming particle and the surface. If the stored elastic energy, Q_E, is greater than the adhesive energy required to separate the particle from the surface, Q'_A, then the particle will rebound otherwise it sticks to the surface. The rebound speed, V_r, is calculated from

$$\tfrac{1}{2}mV_r^2 = Q_E - Q'_A. \tag{3}$$

The mentioned energy terms are described in detail by Rogers and Reed and in van Beek [11]. The maximum

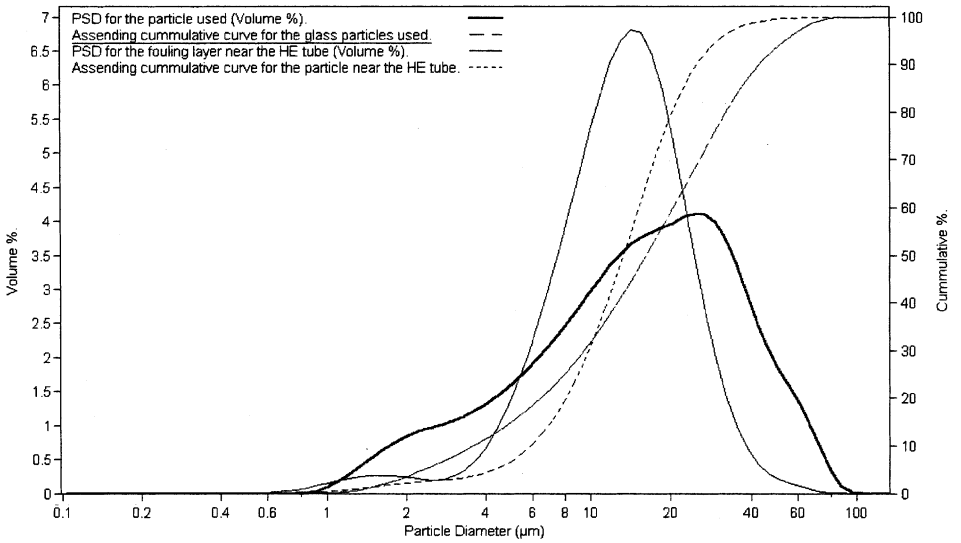

Fig. 12. A comparison between the particle size distribution of the injected glass particles in the airflow and the glass particles in the first fouling layers deposited on the HE tube.

Table 2
A comparison between the particle size distribution of the injected glass particles in the airflow and the glass particles in the first fouling layers deposited on the HE tube

	Mean diameter (d_M)	Standard deviation (SD)	D_{10}[a]	D_{50}[b]	D_{90}[c]
Injected glass particles in airflow	20.4	16.2	3.6	16.2	43.1
Glass particle in the fouling layer near the HE tube	14.7	8.4	5.9	13.3	25.2

All dimensions are in micrometers.
[a] The particle diameter at which 10% of the particles are smaller than it.
[b] The particle diameter at which 50% of the particles are smaller than it.
[c] The particle diameter at which 90% of the particles are smaller than it.

impact speed at which an incident particle will stick to the impacted surface, i.e. $V_r = 0$, is defined as the critical sticking velocity. To show the variation of the sticking velocity with the incident particle diameter the Rogers and Reed model is solved to calculate the sticking velocity for copper particles of diameters 10 and 4 μm hitting a solid steel surface. Fig. 13 shows the variation of the coefficient of restitution, e, with the impact speed, V_{im}, for copper particles of diameters 10 and 4 μm. The coefficient of restitution is defined as the ratio between the normal rebound speed, V_r, and the normal impact speed, V_{im}, for a particle hitting a solid surface. Fig. 13 shows that if a copper particle of diameter 10 μm hits a steel surface at a speed lower than 0.025 m/s it will stick, while a copper particle of diameter 4 μm sticks if it hits at a velocity lower than 0.12 m/s. Therefore, if we have a mixture of particles of diameters 10 and 4 μm in air, which is flowing with an average speed of 1 m/s over a HE tube, there will be a larger number of particles that hit the HE tube with a speed lower than 0.12 m/s than the number of particles that hits with a speed lower than 0.025 m/s. This can explain why small particles are likely to dominate at the beginning of the fouling process.

3.4. Sintering of fouling layers

Once fouling has started and particles accumulate to build up the fouling layer, sintering takes place. Sintering changes the fouling layer structure from a weak powdery layer to a solid stable structure strongly attached to the heat exchanger tubes [12]. Sintering is a function of time and of the hot gas temperature flowing over the fouling layer [13]. Fig. 14 shows a cross sectional view for a fouling layer taken from the previous experiments mentioned above. The particles in the layer are bronze and were subjected to hot air at 200 °C for

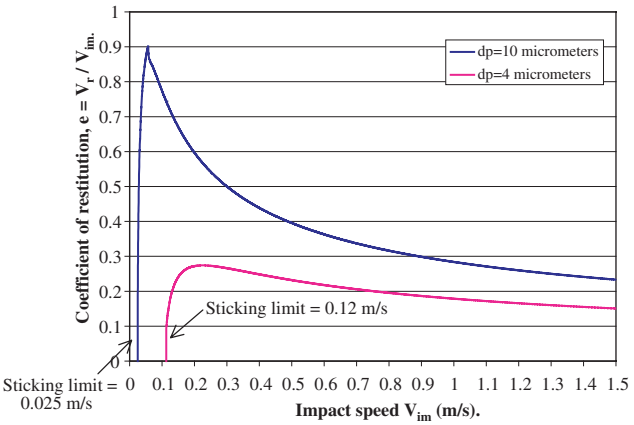

Fig. 13. Coefficient of restitution versus impact speed for copper particles hitting a solid steel surface.

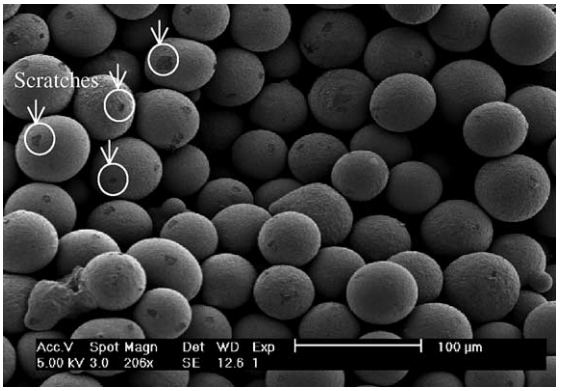

Fig. 14. A cross sectional image through the fouling layer, the arrows show the position of the scratches.

9 h during the fouling experiments. Fig. 2d shows a SEM photo for the bronze particles before usage in the fouling experiments. If we compare Figs. 2d and 14 we find that most of the bronze particles in the fouling layer have scratches on the surface compared to the initial particles. These scratches are probably the areas of contact which have been made up due to sintering and were broken during splitting of the fouling layer for examination under the SEM. Sintering makes removal of the fouling layer by soot blowing afterwards difficult.

4. Concluding discussion

An experimental setup has been built and developed to study the mechanism of fouling over heat exchangers tubes as a function of flow speed and contaminating particles. Fouling starts at areas that are subjected to minimum shearing forces, the rear end of the tubes and then spreads to the circumference due to particle transport to the already deposited particles. Fine particles stick first to the heat exchanger tubes because of their higher sticking velocity than coarse particles. Then the large particles deposit and the fouling layer starts to build up. As the flow speed in the heat exchanger increases, the thickness and the surface area of the fouling layer deposited over the heat exchanger tube are reduced. The flow speed at which fouling ceases is called the limiting fouling speed. The limiting fouling speed is compared to the critical flow velocity required to roll a spherical particle resting on a flat surface and subjected to a shear flow. Depending on the particle size distribution in the gas flow, fine particles deposited on the HE tube may be removed by the large depositing particles. The removal of fine particles by the large depositing particles leads to a lower limiting fouling speed than the limiting fouling speed, which corresponds to the smallest particle in the gas flow. The influence of the particle size distribution on the selection of the limiting fouling speed still has to be investigated in more detail. To prevent fouling, the gas speed of a heat exchanger should be larger than the critical flow velocity that corresponds to the particle size most likely to stick first and remain on the HE tube. As the fouling layer starts to build up sintering takes place. Sintering gradually changes the layer from a loose powdery structure to a more solid structure strongly adhered to the heat exchanger tube. Sintering makes it difficult afterwards to clean the tubes by soot blowing.

Acknowledgements

We would like to acknowledge the staff members of the laboratory of Thermal Engineering at the University of Twente for their assistance in preparing and performing the experiments.

References

[1] J. Taborek, T. Aoki, R.B. Ritter, J.W. Palen, J.G. Knudsen, Fouling: the major unresolved problem in heat transfer, Chem. Eng. Process 68 (2) (1972) 59–67.

[2] H. Müller-Steinhagen, F. Reif, N. Epstein, P. Watkinson, Influence of operating conditions on particulate fouling, Can. J. Chem. Eng. 66 (1988) 42–50.

[3] J.M. Grillot, J. Icart, Fouling of a cylindrical probe and a finned tube bundle in a diesel exhaust environment, Exp. Thermal Fluid Sci. 14 (1997) 442–454.

[4] F.J. Cabrejos, G.F. Klinzing, Incipient motion of solid particles in horizontal pneumatic conveying, Powder Technol. 72 (1992) 51–61.

[5] M.S. Abd-Elhady, C.C.M. Rindt, J.G. Wijers, A.A. van Steenhoven, Removal of particles from powdery fouled surfaces, in: J. Taine (Ed.), Proceedings of the Twelfth International Heat Transfer Conference, Grenoble, France, vol. 2, 2002, pp. 687–692.

[6] M.C. van Beek, C.C.M. Rindt, J.G. Wijers, A.A. van Steenhoven, Analysis of fouling in refuse waste incinerators, Heat Transfer Eng. 22 (2001) 22–31.

[7] L.N. Rogers, J. Reed, The adhesion of particles undergoing an elastic–plastic impact with a surface, J. Phys. D: Appl. Phys. 17 (1984) 677–689.

[8] M. Fichman, D. Pneuli, Sufficient conditions for small particles to hold together because of adhesion forces, ASME J. Appl. Mech. 52 (1985) 105–108.

[9] E. Achenbach, Distribution of local pressure and skin friction around a circular cylinder in cross-flow up to $Re = 5 * 10^6$, J. Fluid Mech. 34 (4) (1968) 625–639.

[10] F. Zhang, A.A. Busnaina, M.A. Fury, S.Q. Wang, The removal of deformed submicron particles from silicon wafers by spin rinse and megasonics, J. Electron. Mater. 29 (2000) 199–204.

[11] M.C. van Beek, Gas-side fouling in heat-recovery boilers, Ph.D. Thesis, Eindhoven University of Technology, Eindhoven, The Netherlands, 2001.

[12] A.L. Robinson, S.G. Buckley, N. Yang, L.L. Baxter, Experimental measurements of the thermal conductivity of ash deposits: Part 2. Effects of sintering and deposit microstructure, Energy Fuels 15 (2001) 15–84.

[13] H.R. Rezaei, R.P. Gupta, G.W. Bryant, J.T. Hart, G.S. Liu, C.W. Bailey, T.F. Wall, S. Miyamae, K. Makino, Y. Endo, Thermal conductivity of coal ash and slags and models used, Fuel 79 (2000) 1697–1710.